

# Spin dephasing in $n$ -typed GaAs quantum wells

M. Q. Weng<sup>a,b</sup>, T. Rao<sup>b</sup>, M. W. Wu<sup>a,b,\*</sup>, and M. Ning<sup>b</sup>

<sup>a</sup>Structure Research Laboratory, University of Science & Technology of China, Academia Sinica, Hefei, Anhui, 230026, China

<sup>b</sup>Department of Physics, University of Science & Technology of China, Hefei, Anhui, 230026, China<sup>\*\*</sup>

(November 30, 2019)

We perform a many-body study of the spin dephasing due to the D'yakonov-Perel' effect in  $n$ -typed GaAs (100) quantum wells under moderate magnetic fields in the Voigt configuration by constructing and numerically solving the kinetic Bloch equations. We include all the spin conserving scattering such as electron-phonon, the electron-nonnagnetic impurity as well as the electron-electron Coulomb scattering in our theory and investigate how the spin dephasing time (SDT) is affected by the initial spin polarization, temperature, impurity, magnetic field as well as the electron density. The dephasing obtained from our theory contains not only that due to the effective spin-flipping scattering first proposed by D'yakonov and Perel' [Zh. Eksp. Teor. Fiz. **60**, 1954(1971)[Sov. Phys.-JETP **38**, 1053(1971)]], but also the recently proposed many-body dephasing due to the inhomogeneous broadening provided by the DP term [Wu, J. Supercond.:Incorp. Novel Mechanism **14**, 245 (2001); Wu and Ning, Eur. Phys. J. B **18**, 373 (2000)]. We show that for the electron densities we study, the SDT is dominated by the many-body effect. Equally remarkable is that we are now able to investigate the spin dephasing with extra large spin polarization (up to 100 %) which has not been discussed both theoretically and experimentally. We find a huge anomalous resonance of the SDT for large spin polarizations. The SDT we get at low initial spin polarization is in agreement with the experiment data both qualitatively and quantitatively.

PACS: 71.10.-w, 67.57.Lm, 72.25.Rb, 73.61.Ey

## I. INTRODUCTION

The resent development of ultrafast nonlinear optical experiments<sup>1,2,3,4,5,6,7,8,9,10,11,12</sup> has stimulated immense interest in spintronics in semiconductors as it shows great potential of using the spin degree of freedom of electrons in place of/in addition to the charge degree of freedom for device application such as qubits, quantum memory devices, and spin transistors.

In order to make use of the spin degree of freedom in semiconductor spintronics, it is crucial to have a thorough understanding of spin dephasing mechanism. Three spin dephasing mechanisms have been proposed in semiconductors:<sup>13,14</sup> the Ellit-Yafet (EY) mechanism,<sup>15,16</sup> the D'yakonov-Perel' (DP) mechanism,<sup>17</sup> and the Bir-Aronov-Pikus (BAP) mechanism.<sup>18</sup> In the EY mechanism, the spin-orbit interaction leads to mixing of wave functions of opposite spins. This mixing results in a nonzero electron spin flip due to impurity and phonon scattering. The DP mechanism is due to the spin-orbit interaction in crystals without inversion center, which results in spin state splitting of the conduction band at  $k \neq 0$ . This is equivalent to an effective magnetic field acting on the spin, with its magnitude and orientation depending on  $\mathbf{k}$ . Finally, the BAP mechanism is originated from the mixing of heavy hole and light hole bands induces by spin-orbit coupling. Spin-flip (SF) scattering of electrons by holes due to the Coulomb interaction is therefore permitted, which gives rise to spin dephasing. The dephasing rates of these mechanisms for low polarized system are calculated in the framework of single particle approximation.<sup>13</sup> For GaAs, the EY mech-

anism is less effective under most conditions, due to the large band gap and low scattering rate for high quality samples. The BAP mechanism is important for either  $p$ -doped or insulating GaAs. For  $n$ -doped samples, however, as holes are rapidly recombined with electrons due to the presence of a large number of electrons, spin dephasing due to the regular BAP mechanism is blocked. Therefore, the DP mechanism (or possibly the EY mechanism under certain conditions) is the main mechanism of spin dephasing for  $n$ -type GaAs.

It is important to note that all the mechanisms above either provide or are treated as SF scattering. Spin-conserving (SC) scattering, such as the ordinary Coulomb scattering, electron-phonon and electron-nonnagnetic impurity scattering which has been extensively studied in connection with optical dephasing and relaxation,<sup>19</sup> are commonly believed to be unable to cause spin dephasing as the corresponding interaction Hamiltonians commute with the total spin operator.

Recently Wu presented a many-body kinetic theory to study the spin precession and spin dephasing in insulating ZnSe/Zn<sub>1-x</sub>Cd<sub>x</sub>Se quantum well (QW),<sup>20</sup>  $n$ -typed bulk GaAs samples,<sup>21</sup> and  $n$ -typed GaAs (110) QW,<sup>22</sup> under moderate magnetic fields in the Voigt configuration. Based on this many-body theory, he further showed that the SC scattering can also cause spin dephasing in the presence of inhomogeneous broadening.<sup>20,21,22,23,24,25</sup> This novel spin dephasing mechanism has long been overlooked in the literature. Differing from the earlier study of the spin dephasing which comes from SF scattering, the spin dephasing through inhomogeneous broadening is caused by irreversibly disrupting the phases between

spin dipoles and is therefore a many-body effect.<sup>23,24,25</sup>

In this paper, we study the spin dephasing in  $n$ -doped GaAs (100) QW's. We calculate the SDT by numerically solving the many-body kinetic equations with all the scattering included. Differing from the previous investigation in the bulk case where we are only able to get the SDT qualitatively,<sup>21</sup> here we get the SDT quantitatively thanks to the reduction of dimension in the momentum space. Moreover as we include the electron-electron Coulomb scattering in our calculation, for the first time we are able to study the spin dephasing with extra large initial spin polarization (up to 100 %) which has not been investigated both experimentally and theoretically.

We organize the paper as follows: We present our model and the kinetic equations in Sec. II. Then in Sec. III(A) we show the time evolution of the spin signal where we show the contribution of the Coulomb scattering to the spin dephasing. In Sec. III(B) we investigate how the SDT changes with the variation of the initial spin polarization. The temperature dependence of the SDT under different spin polarization is discussed in detail in Sec. III(C), where we also highlight the difference between the present many-body theory and the earlier simplified theory. In Sec. III(D) we show the magnetic field dependence of the SDT. Finally we discuss how the electron density affect the SDT. We present the conclusion and summary in Sec. IV.

## II. KINETIC EQUATIONS

We start our investigation from an  $n$ -doped (100) GaAs QW with well width  $a$ . The growth direction is assumed to be  $z$ -axis. A moderate magnetic field  $\mathbf{B}$  is applied along the  $x$  axis. Due to the confinement of the QW, the momentum states along  $z$  axis are quantized. Therefore the electron states are characterized by a subband index  $n$  and a two dimensional wave vector  $\mathbf{k} = (k_x, k_y)$  together with a spin index  $\sigma$ . In the present paper, the subband separation is assumed to be large enough so that only the lowest subband is populated and the transition to the upper subbands is unimportant. Therefore, one only needs to consider the lowest subband. For  $n$ -doped samples, spin dephasing mainly comes from the DP mechanism.<sup>17</sup> With the DP term included, the Hamiltonian of the electrons in the QW takes the form:

$$H = \sum_{\mathbf{k}\sigma\sigma'} \left\{ \varepsilon_{\mathbf{k}} + [g\mu_B \mathbf{B} + \mathbf{h}(\mathbf{k})] \cdot \frac{\vec{\sigma}_{\sigma\sigma'}}{2} \right\} c_{\mathbf{k}\sigma}^\dagger c_{\mathbf{k}\sigma'} + H_I. \quad (1)$$

Here  $\varepsilon_{\mathbf{k}} = \mathbf{k}^2/2m^*$  is the energy of electron with wavevector  $\mathbf{k}$  and effective mass  $m^*$ .  $\vec{\sigma}$  are the Pauli matrices. In QW system, the DP term is composed of the Dresselhaus term<sup>26</sup> and the Rashba term.<sup>27,28</sup> The Dresselhaus term is due to the lack of inversion symmetry in the zinc-blende crystal Brillouin zone and is sometimes referred to as bulk inversion asymmetry (BIA) term. For the (100) GaAs QW system, it can be written as<sup>29,30</sup>

$$\begin{aligned} h_x^{\text{BIA}}(\mathbf{k}) &= \gamma k_x (k_y^2 - \langle k_z^2 \rangle), \\ h_y^{\text{BIA}}(\mathbf{k}) &= \gamma k_y (\langle k_z^2 \rangle - k_x^2), \\ h_z^{\text{BIA}}(\mathbf{k}) &= 0. \end{aligned} \quad (2)$$

Here  $\langle k_z^2 \rangle$  represents the average of the operator  $-(\frac{\partial}{\partial z})^2$  over the electronic state of the lowest subband and is therefore  $(\pi/a)^2$ .  $\gamma = (4/3)(m^*/m_{cv})(1/\sqrt{2m^*E_g})(\eta/\sqrt{1-\eta/3})$  and  $\eta = \Delta/(E_g + \Delta)$ , in which  $E_g$  denotes the band gap;  $\Delta$  represents the spin-orbit splitting of the valence band;  $m^*$  standing for the electron mass in GaAs; and  $m_{cv}$  is a constant close in magnitude to free electron mass  $m_0$ .<sup>14</sup> Whereas the Rashba term appears if the self-consistent potential within a QW is asymmetric along the growth direction and is therefore referred to as structure inversion asymmetry (SIA) contribution. Its scale is proportional to the interface electric field along the growth direction. For narrow band-gap semiconductors such as InAs, the Rashba term is the main spin-dephasing mechanism; whereas in the wide band-gap semiconductors such as GaAs, the Dresselhaus term is dominant. In the present paper, we will take only the Dresselhaus term into consideration as we focus on the spin dephasing in GaAs QW. The interaction Hamiltonian  $H_I$  is composed of Coulomb interaction  $H_{ee}$ , electron-phonon interaction  $H_{ph}$ , as well as electron-impurity scattering  $H_i$ . Their expressions can be found in textbooks.<sup>19,31</sup>

We construct the kinetic Bloch equations by the nonequilibrium Green function method<sup>19</sup> as follows:

$$\dot{\rho}_{\mathbf{k},\sigma\sigma'} = \dot{\rho}_{\mathbf{k},\sigma\sigma'}|_{\text{coh}} + \dot{\rho}_{\mathbf{k},\sigma\sigma'}|_{\text{scatt}} \quad (3)$$

Here  $\rho_{\mathbf{k}}$  represents the single particle density matrix. The diagonal elements describe the electron distribution functions  $\rho_{\mathbf{k},\sigma\sigma} = f_{\mathbf{k}\sigma}$ . The off-diagonal elements  $\rho_{\mathbf{k},\frac{1}{2}-\frac{1}{2}} \equiv \rho_{\mathbf{k}}$  describe the inter-spin-band polarizations (coherence) of the spin coherence.<sup>20</sup> Note that  $\rho_{\mathbf{k},-\frac{1}{2}\frac{1}{2}} \equiv \rho_{\mathbf{k},\frac{1}{2}-\frac{1}{2}}^* = \rho_{\mathbf{k}}^*$ . Therefore,  $f_{\mathbf{k}\pm\frac{1}{2}}$  and  $\rho_{\mathbf{k}}$  are the quantities to be determined from Bloch equations.

The coherent part of the equation of motion for the electron distribution function is given by

$$\frac{\partial f_{\mathbf{k},\sigma}}{\partial t}|_{\text{coh}} = -2\sigma \{ [g\mu_B B + h_x(\mathbf{k})] \text{Im} \rho_{\mathbf{k}} + h_y(\mathbf{k}) \text{Re} \rho_{\mathbf{k}} \} + 4\sigma \text{Im} \sum_{\mathbf{q}} V_{\mathbf{q}} \rho_{\mathbf{k}+\mathbf{q}}^* \rho_{\mathbf{k}}, \quad (4)$$

where  $V_{\mathbf{q}} = 4\pi e^2/[\kappa_0(q + q_0)]$  is the 2D Coulomb matrix element under static screening.  $q_0 = (2e^2 m^* / \kappa_0) \sum_{\sigma} f_{\mathbf{k}=0,\sigma}$

and  $\kappa_0$  is the static dielectric constant. The first term on the right hand side (RHS) of Eq. (4) describes spin precession of electrons under the magnetic field  $\mathbf{B}$  as well as the effective magnetic field  $\mathbf{h}(\mathbf{k})$  due to the DP effect. The scattering terms of electron distribution functions in the Markovian limit are given by

$$\begin{aligned} \frac{\partial f_{\mathbf{k},\sigma}}{\partial t}|_{\text{scatt}} = & \left\{ -2\pi \sum_{\mathbf{q}q_z\lambda} g_{\mathbf{Q}\lambda}^2 \delta(\varepsilon_{\mathbf{k}} - \varepsilon_{\mathbf{k}-\mathbf{q}} - \Omega_{\mathbf{q}q_z\lambda}) [N_{\mathbf{q}q_z\lambda} (f_{\mathbf{k}\sigma} - f_{\mathbf{k}-\mathbf{q}\sigma}) + f_{\mathbf{k}\sigma} (1 - f_{\mathbf{k}-\mathbf{q}\sigma}) - \text{Re}(\rho_{\mathbf{k}} \rho_{\mathbf{k}-\mathbf{q}}^*)] \right. \\ & - 2\pi N_i \sum_{\mathbf{q}} U_{\mathbf{q}}^2 \delta(\varepsilon_{\mathbf{k}} - \varepsilon_{\mathbf{k}-\mathbf{q}}) [f_{\mathbf{k}\sigma} (1 - f_{\mathbf{k}-\mathbf{q}\sigma}) - \text{Re}(\rho_{\mathbf{k}} \rho_{\mathbf{k}-\mathbf{q}}^*)] - 2\pi \sum_{\mathbf{q}\mathbf{k}'\sigma'} V_{\mathbf{q}}^2 \delta(\varepsilon_{\mathbf{k}-\mathbf{q}} - \varepsilon_{\mathbf{k}} + \varepsilon_{\mathbf{k}'} - \varepsilon_{\mathbf{k}'-\mathbf{q}}) \\ & \left. \left[ (1 - f_{\mathbf{k}-\mathbf{q}\sigma}) f_{\mathbf{k}\sigma} (1 - f_{\mathbf{k}'\sigma'}) f_{\mathbf{k}'-\mathbf{q}\sigma'} + \frac{1}{2} \rho_{\mathbf{k}} \rho_{\mathbf{k}-\mathbf{q}}^* (f_{\mathbf{k}'\sigma'} - f_{\mathbf{k}'-\mathbf{q}\sigma'}) + \frac{1}{2} \rho_{\mathbf{k}'} \rho_{\mathbf{k}'-\mathbf{q}}^* (f_{\mathbf{k}-\mathbf{q}\sigma} - f_{\mathbf{k}\sigma}) \right] \right\} \\ & - \{\mathbf{k} \leftrightarrow \mathbf{k} - \mathbf{q}, \mathbf{k}' \leftrightarrow \mathbf{k}' - \mathbf{q}\}, \end{aligned} \quad (5)$$

in which  $\{\mathbf{k} \leftrightarrow \mathbf{k} - \mathbf{q}, \mathbf{k}' \leftrightarrow \mathbf{k}' - \mathbf{q}\}$  stands for the same terms as in the previous  $\{\}$  but with the interchange  $\mathbf{k} \leftrightarrow \mathbf{k} - \mathbf{q}$  and  $\mathbf{k}' \leftrightarrow \mathbf{k}' - \mathbf{q}$ . The first term inside the braces on the RHS of Eq. (5) comes from the electron-phonon interaction.  $\lambda$  stands for the different phonon modes, *i.e.*, one longitude optical (LO) phonon mode, one longitudinal acoustic (AC) phonon mode due to the deformation potential, and two AC modes due to the transverse piezoelectric field.  $g_{\mathbf{q}q_z\lambda}$  are the matrix elements of electron-phonon coupling for mode  $\lambda$ . For LO phonons,  $g_{\mathbf{q}q_z\text{LO}}^2 = \{4\pi\alpha\Omega_{\text{LO}}^{3/2}/[\sqrt{2\mu}(q^2 + q_z^2)]\}|I(iq_z)|^2$  with  $\alpha = e^2\sqrt{\mu/(2\Omega_{\text{LO}})}(\kappa_{\infty}^{-1} - \kappa_0^{-1})$ .  $\kappa_{\infty}$  is the optical dielectric constant and  $\Omega_{\text{LO}}$  is the LO phonon frequency. The form

factor  $|I(iq_z)|^2 = \pi^2 \sin^2 y/[y^2(y^2 - \pi^2)^2]$  with  $y = q_z a/2$ .  $N_{\mathbf{q}q_z\lambda} = 1/[\exp(\Omega_{\mathbf{q}q_z\lambda}/k_B T) - 1]$  is the Bose distribution of phonon mode  $\lambda$  at temperature  $T$ . The second term inside the braces on the RHS of Eq. (5) results from the electron-impurity scattering under the random phase approximation with  $N_i$  denoting the impurity concentration.  $U_{\mathbf{q}}^2 = \sum_{q_z} \{4\pi Z_i e^2/[\kappa_0(q^2 + q_z^2)]\}^2 |I(iq_z)|^2$  is the electron-impurity interaction matrix element with  $Z_i$  stands for the charge number of the impurity.  $Z_i$  is assumed to be 1 throughout our calculation. The third term is the contribution of the Coulomb interaction. Similarly, the coherent and the scattering parts of the spin coherence are given by

$$\frac{\partial \rho_{\mathbf{k}}}{\partial t}|_{\text{coh}} = \frac{1}{2} [ig\mu_B B + ih_x(\mathbf{k}) + h_y(\mathbf{k})] (f_{\mathbf{k}\frac{1}{2}} - f_{\mathbf{k}-\frac{1}{2}}) + i \sum_{\mathbf{q}} V_{\mathbf{q}} [(f_{\mathbf{k}+\mathbf{q}\frac{1}{2}} - f_{\mathbf{k}+\mathbf{q}-\frac{1}{2}}) \rho_{\mathbf{k}} - \rho_{\mathbf{k}+\mathbf{q}} (f_{\mathbf{k}\frac{1}{2}} - f_{\mathbf{k}-\frac{1}{2}})], \quad (6)$$

$$\begin{aligned} \frac{\partial \rho_{\mathbf{k}}}{\partial t}|_{\text{scatt}} = & \left\{ \pi \sum_{\mathbf{q}q_z\lambda} g_{\mathbf{q}q_z\lambda}^2 \delta(\varepsilon_{\mathbf{k}} - \varepsilon_{\mathbf{k}-\mathbf{q}} - \Omega_{\mathbf{q}q_z\lambda}) [\rho_{\mathbf{k}-\mathbf{q}} (f_{\mathbf{k}\frac{1}{2}} + f_{\mathbf{k}-\frac{1}{2}}) + (f_{\mathbf{k}-\mathbf{q}\frac{1}{2}} + f_{\mathbf{k}-\mathbf{q}-\frac{1}{2}} - 2) \rho_{\mathbf{k}} - 2N_{\mathbf{q}q_z\lambda} (\rho_{\mathbf{k}} - \rho_{\mathbf{k}-\mathbf{q}})] \right. \\ & + \pi N_i \sum_{\mathbf{q}} U_{\mathbf{q}}^2 \delta(\varepsilon_{\mathbf{k}} - \varepsilon_{\mathbf{k}-\mathbf{q}}) [(f_{\mathbf{k}\frac{1}{2}} + f_{\mathbf{k}-\frac{1}{2}}) \rho_{\mathbf{k}-\mathbf{q}} - (2 - f_{\mathbf{k}-\mathbf{q}\frac{1}{2}} - f_{\mathbf{k}-\mathbf{q}-\frac{1}{2}}) \rho_{\mathbf{k}}] \\ & - \sum_{\mathbf{q}\mathbf{k}'} \pi V_{\mathbf{q}}^2 \delta(\varepsilon_{\mathbf{k}-\mathbf{q}} - \varepsilon_{\mathbf{k}} + \varepsilon_{\mathbf{k}'} - \varepsilon_{\mathbf{k}'-\mathbf{q}}) \left( (f_{\mathbf{k}-\mathbf{q}\frac{1}{2}} \rho_{\mathbf{k}} + \rho_{\mathbf{k}-\mathbf{q}} f_{\mathbf{k}-\frac{1}{2}}) (f_{\mathbf{k}'\frac{1}{2}} - f_{\mathbf{k}'-\mathbf{q}\frac{1}{2}} + f_{\mathbf{k}'-\frac{1}{2}} - f_{\mathbf{k}'-\mathbf{q}-\frac{1}{2}}) \right. \\ & + \rho_{\mathbf{k}} [(1 - f_{\mathbf{k}'\frac{1}{2}}) f_{\mathbf{k}-\mathbf{q}\frac{1}{2}} + (1 - f_{\mathbf{k}'-\frac{1}{2}}) f_{\mathbf{k}-\mathbf{q}-\frac{1}{2}} - 2\text{Re}(\rho_{\mathbf{k}'}^* \rho_{\mathbf{k}-\mathbf{q}})] - \rho_{\mathbf{k}-\mathbf{q}} [f_{\mathbf{k}'\frac{1}{2}} (1 - f_{\mathbf{k}'-\mathbf{q}\frac{1}{2}}) \\ & \left. \left. + (1 - f_{\mathbf{k}'-\frac{1}{2}}) f_{\mathbf{k}'-\mathbf{q}-\frac{1}{2}} - 2\text{Re}(\rho_{\mathbf{k}'}^* \rho_{\mathbf{k}'-\mathbf{q}})] \right) \right\} - \{\mathbf{k} \leftrightarrow \mathbf{k} - \mathbf{q}, \mathbf{k}' \leftrightarrow \mathbf{k}' - \mathbf{q}\}. \end{aligned} \quad (7)$$

The initial conditions are taken at  $t = 0$  as:

$$\rho_{\mathbf{k}}|_{t=0} = 0 \quad (8)$$

$$f_{\mathbf{k}\sigma}|_{t=0} = 1/\{\exp[(\varepsilon_{\mathbf{k}} - \mu_{\sigma})/k_B T] + 1\} \quad (9)$$

where  $\mu_{\sigma}$  is the chemical potential for spin  $\sigma$ . The condition  $\mu_{\frac{1}{2}} \neq \mu_{-\frac{1}{2}}$  gives rise to the imbalance of the electron densities of the two spin bands. Eqs. (3) through

(7) together with the initial conditions Eqs. (8) and (9) comprise the complete set of kinetic Bloch equations of our investigation.

### III. NUMERICAL RESULTS

The kinetic Bloch equations form a set of nonlinear equations. All the unknowns to be solved appear in the

scattering terms. Specifically, the electron distribution function is no longer a Fermi distribution because of the existence of the anisotropic DP term  $\mathbf{h}(\mathbf{k})$ . This term in the coherent part drives the electron distribution away from an isotropic Fermi distribution. The scattering term attempts to randomize electrons in  $\mathbf{k}$ -space. Obviously, both the coherent part and the scattering terms have to be solved self-consistently to obtain the distribution function and the spin coherence.

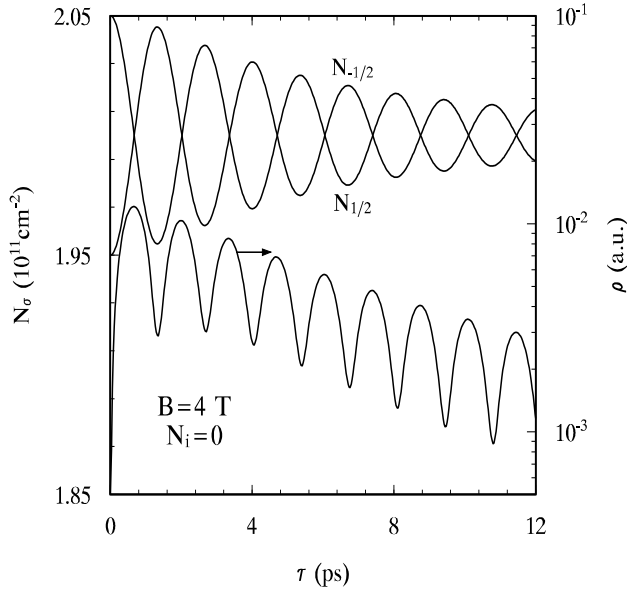


FIG. 1. Electron densities of up spin and down spin and the incoherently summed spin coherence  $\rho$  versus time  $t$  without taking account the Coulomb scattering for a GaAs QW with initial spin polarization  $P = 2.5\%$ , at  $T = 200$  K. Note the scale of the spin coherence is on the right side of the figure.

We numerically solve the kinetic Bloch equations in such a self-consistent fashion to study the spin precession between the spin-up and -down bands. We include electron-phonon scattering and the electron-electron interaction throughout our computation. As we concentrate on the relatively high temperature regime in the present study, for electron-phonon scattering we only need to include electron-LO phonon scattering. Electron-impurity scattering is sometimes excluded. As discussed in the previous paper,<sup>20,32</sup> irreversible spin dephasing can be well defined by the slope of the envelope of the incoherently summed spin coherence  $\rho(t) = \sum_{\mathbf{k}} |\rho_{\mathbf{k}}|$ . The material parameters of GaAs for our calculation are tabulated in Table I.<sup>33</sup> It is noted that in two-dimensional systems the Landé  $g$ -factor for the in-plane magnetic field is greatly enhanced compared with that of bulk value.<sup>34,35,36,37,38</sup> Here we choose the  $g$ -factor to be 6.5 which is near the experiment data of Nicholas *et al.*<sup>37</sup> instead of 0.44 commonly used in the bulk GaAs system.<sup>39</sup> The method of the numerical calculation has been laid out in detail in our previous paper on the DP mechanism

in 3D systems.<sup>21</sup> The difference is that here we are able to get the results quantitatively instead of only qualitatively as in our previous 3D case, thanks to the smaller dimension in the momentum space. Our main results are plotted in Figs. 1 to 8. In these calculations the total electron density  $N_e$  and the applied magnetic field  $B$  are chose to be  $4 \times 10^{11} \text{ cm}^{-2}$  and 4 T respectively unless otherwise specified.

### A. Temporal evolution of the spin signal

We first study the temporal evolution of the spin signal in a GaAs QW at  $T = 200$  K. In Fig. 1 we plot the electron densities in the spin-up and -down bands together with the incoherently summed spin coherence for  $N_i = 0$ . At  $t = 0$ , the initial spin polarization  $P = (N_{1/2} - N_{-1/2})/(N_{1/2} + N_{-1/2})$  is 2.5%. In this calculation, the Coulomb scattering is not included. It is seen from the figure that excess electrons in the spin-up band start to flip to the spin-down band at  $t = 0$  due to the presence of the magnetic field and the DP term  $\mathbf{h}(\mathbf{k})$ . In the meantime the spin coherence  $\rho$  accumulates. At about 0.67 ps, the electron densities in the two spin bands become equal and the spin coherence reaches its maximum. Then the spin coherence starts to feed back and the electron density in the spin-down band exceeds that in the spin-up band while  $\rho$  deceases. At about 1.3 ps,  $\rho$  reach its minimum, while the density difference in the two spin bands reaches its maximum again with the excess electrons now in the spin-down band. Due to the dephasing, the second peak is lower than the first one. This oscillation goes on until the amplitude of the oscillation becomes zero due to the dephasing.

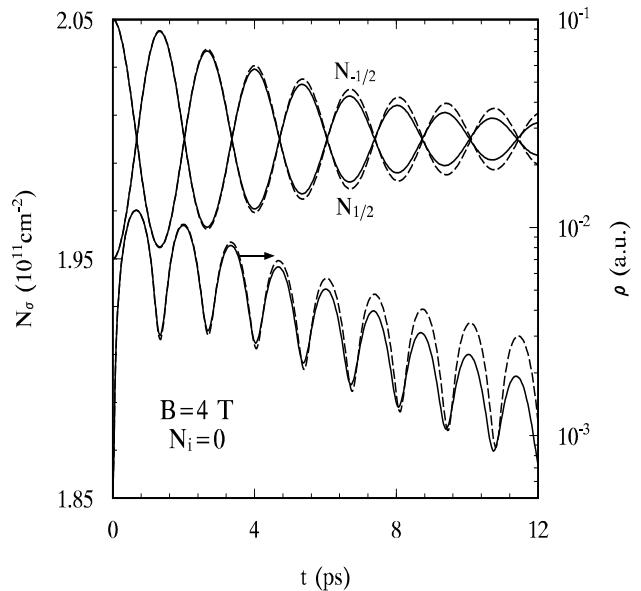


FIG. 2. Electron densities of up spin and down spin and the incoherently summed spin coherence  $\rho$  versus time  $t$  with (solid curves) and without (dashed curves) taking account the Coulomb scattering for a GaAs QW initial spin polarization  $P = 2.5\%$  at  $T = 200$  K. Note the scale of the spin coherence is on the right side of the figure.

In Fig. 2, we plot the time evolution of electron densities in the two spin bands as well as the incoherently summed spin coherence for the same GaAs QW system as the previous one but taking the Coulomb scattering into account. The results without the Coulomb scattering are replotted as dashed curves in the figure. It is seen from the figure that for the first three oscillations ( $t < 4$  ps), the electron densities as well as the spin coherences are almost the same in the presence and absence of the Coulomb scattering. As time goes on, the curves with the Coulomb scattering deviate from the ones without the Coulomb scattering. The decay rates of the excess spin density as well as the spin coherence are faster in the presence of Coulomb scattering.

It is known that, the Coulomb scattering is important only when the electron distribution is divagated from the Fermi function. In the first few picoseconds, the electrons in the two spin bands flip to their opposite bands due to the magnetic fields. The buildup of the inhomogeneity of  $\mathbf{k}$  in the electron distribution function comes from the DP term is marginal, and the electron distributions remain approximately the Fermi function. As time goes on, the effect of the DP term accumulates, the electron distribution functions divagate further and further away from the Fermi function and hence the Coulomb scattering becomes more and more important. Consequently, the spin signal that with the Coulomb scattering differs from the one without the Coulomb scattering. It has been pointed out that the spin dephasing due to the DP term and the SC scattering comes from two effects.<sup>21</sup> The first one is widely discussed which is due to the anisotropic property of the DP term, which, combined with SC scattering gives rise to the effective SF scattering.<sup>13,17</sup> In this case, inclusion of additional scattering enhances the momentum relaxation rate and consequently reduces the spin dephasing rate.<sup>13,17,23</sup> It has been pointed out that the electron-electron Coulomb scattering, although does not contribute to the momentum relaxation rate, trends to reduce the spin dephasing<sup>40</sup> based on the similar analysis as in Refs. 13, 17, 23. The second is that the DP term itself also introduces an inhomogeneous broadening, which in the presence of the SC scattering provides *additional* spin dephasing channel<sup>21,22,23,24,25</sup> and therefore results a faster spin dephasing. Our calculation self-consistently solves the Kinetic Bloch equations and includes both effects. The result indicates that for the present condition the second effect is more important and therefore the combined effect by inclusion of the Coulomb scattering leads to the increase of the spin dephasing.

## B. Spin polarization dependence of the spin dephasing time

We now turn to study the spin polarization dependence of the SDT. As our theory is a many-body theory and we include all the scatterings, especially the Coulomb scattering, in our calculation, we are able to calculate the SDT with large spin polarization.

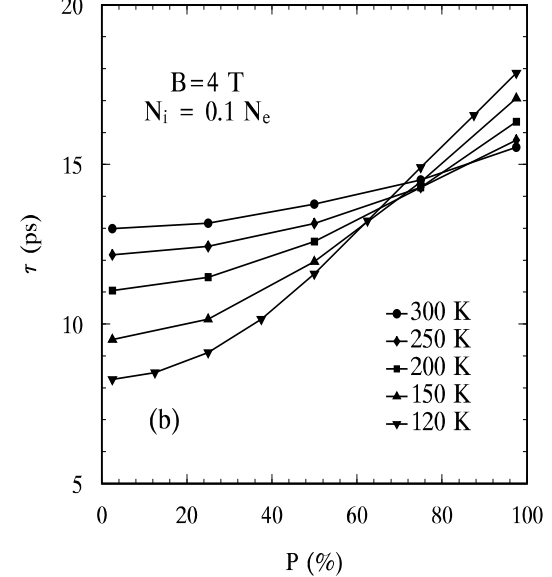
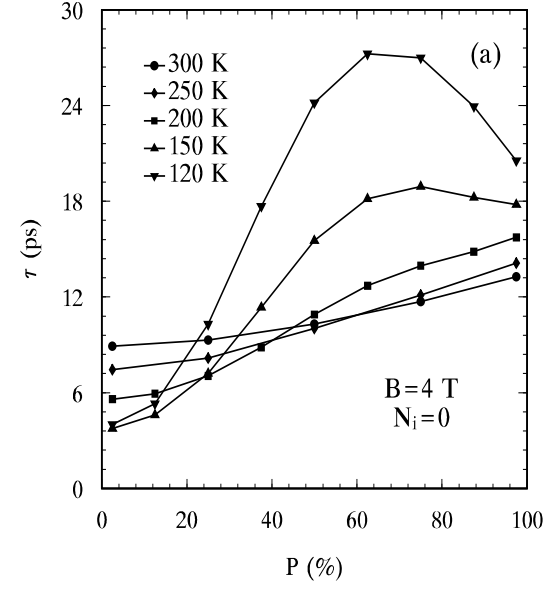


FIG. 3. Spin dephasing time  $\tau$  versus the initial spin polarization  $P$  for a GaAs QW with different impurity concentration and different temperatures. Down triangle (▼):  $T = 120$  K; Up triangle (▲):  $T = 150$  K; Square (■):  $T = 200$  K; Diamond (◆):  $T = 250$  K; Circle (●):  $T = 300$  K. The impurity densities in (a) and (b) are 0 and  $0.1N_e$  respectively. The lines are plotted for the aid of eyes.

In Fig. 3, SDT  $\tau$  is plotted against the initial spin polarization  $P$  for GaAs QW's with  $N_i = 0$  [Fig. 3(a)] and  $N_i = 0.1N_e$  [Fig. 3(b)] at different temperatures. The most striking feature of the impurity-free case is the huge anomalous peaks of the SDT in low temperatures. For  $T = 120$  K, the peak value of the SDT is about 6 times higher than that of low initial spin polarization. It is also seen from the figure that the anomalous peak is reduced with the increase of temperature and the peak shifts to higher polarization. For  $T > 200$  K there is no anomalous peak.

The anomalous peak in the  $\tau$ - $P$  curve in low temperature region originates from the electron-electron interaction, specifically the Hartree-Fock (HF) self-energy [*i.e.*, the last terms in the Eq. (4) and (6)]. As we know that the HF term itself does not contribute to the spin dephasing directly.<sup>24,25</sup> However, it can alert the motion of the electrons and can therefore affect the spin dephasing by combining with the DP term. For small spin polarization as commonly discussed in the literature, the contribution of the HF term is marginal. However, when the polarization gets higher, the HF contribution becomes larger. Under the right polarization, it may reach the magnitude comparable to the contribution from the DP term as well as the applied magnetic field in the coherent parts of the Bloch equations and reduces the anisotropic caused by the DP term. Therefore, one gets longer SDT. It is noted that this anomalous peak is similar to the resonance effect. As both the DP term and the HF term are  $k$ -dependent, the resonance is broadened. However, if one further increases the initial polarization, the HF term exceeds the resonance condition. As the result, the SDT decreases. If one removes the HF term, the anomalous resonance as well as the large increase of SDT disappears.

For high temperatures the HF term is smaller. In order to reach the resonance, one needs to go to higher polarization. Therefore, as shown in the figure the anomalous peak shifts to the higher polarization. However, when the temperature is high enough, even largest polarization  $P = 100$  % cannot make the HF term to reach the resonance condition. Therefore, the peak disappears.

The  $\tau$ - $P$  curve is much different when the impurities are introduced. It is seen from Fig. 3(b) that, when the density of impurity is large, say  $N_i = 0.1N_e$ , the fast rise in  $\tau$ - $P$  curve remains. Nevertheless the increase is much smaller than the corresponding one when the impurities are absent. In addition to the reduction of the rise in  $\tau$ - $P$  curves, the impurities destroy the anomaly too. One can easily see that, with the impurity level  $N_i = 0.1N_e$ , for all of the temperatures we study, the SDT increases uniquely with the polarization.

To further reveal the contribution of the impurity to the dephasing under different conditions, we plot the SDT as a function of the polarization for different impurity levels at  $T = 120$  K and 200 K in Fig. 4(a) and (b) respectively. The figure clearly shows that for low temperature, the impurity tends to remove the anomalous peak and to shift the peak to the larger initial spin

polarization. This is because that the impurity reduces the HF term and therefore the resonance effect is also reduced. Hence, in order to reach the maximum resonance, one has to increase the initial spin polarization. Consequently, the peak shifts to larger  $P$ . Whereas when  $N_i$  is raised to  $0.1N_e$ , the HF term is reduced too much to form a peak. It is also noted that for high temperatures, there is no anomalous peak.

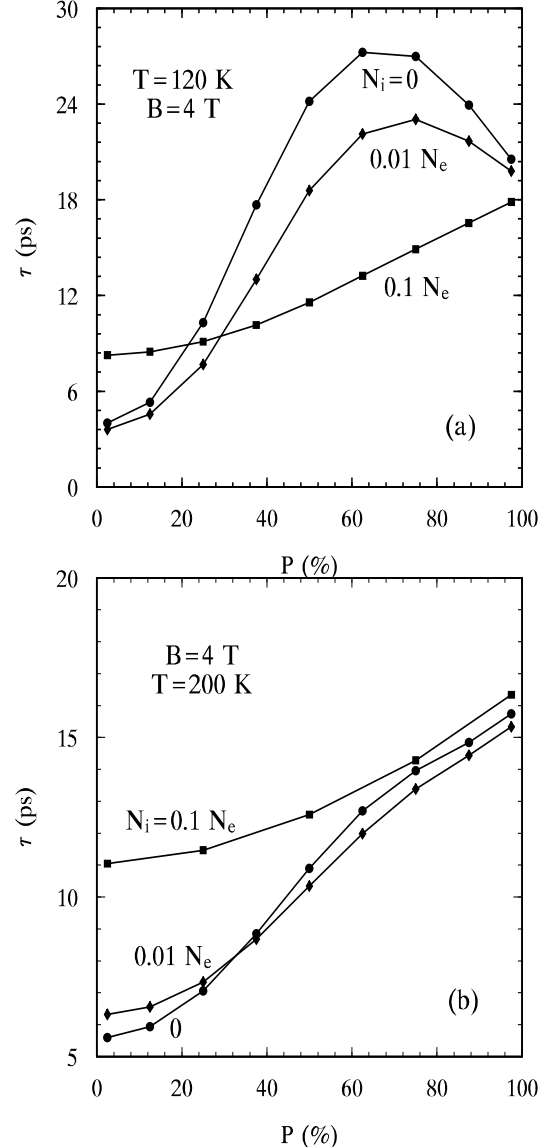


FIG. 4. Spin dephasing time  $\tau$  versus the initial spin polarization  $P$  for a GaAs QW with different impurity levels. Circle ( $\bullet$ ):  $N_i = 0$ ; Diamond ( $\blacklozenge$ ):  $N_i = 0.01N_e$ ; Square ( $\blacksquare$ ):  $N_i = 0.1N_e$ . The lines are plotted for the aid of eyes.

It is interesting to note that in the low polarized regime and when the temperature is 120 K,  $\tau$  first decreases when the impurities are introduced. However, when we further increase the impurity level from  $N_i = 0.01N_e$  to  $N_i = 0.1N_e$ ,  $\tau$  increases again. As we pointed out be-

fore that the impurities affect the spin dephasing in two ways.<sup>21</sup> On one hand, the electron-impurity scattering provides a new spin dephasing channel through combining with the DP term<sup>17,21</sup> to give an effective SF scattering and through the inhomogeneous broadening provided by the DP term.<sup>21,22,23,24,25</sup> This gives rise to the enhancement of the dephasing. On the other hand, the scattering also redistributes the electrons in the momentum space and leads them to an isotropic distribution. Therefore, the scattering can suppress the anisotropy caused by the DP term, consequently the effective spin-flipping scattering. This leads to a smaller spin dephasing. Our result indicates that in low temperature and low polarization region, the impurities tend to reduce the SDT through the added spin dephasing channel when their concentration is small. When the impurity level increases, the impurities destroy the anisotropy introduced by DP effect more effectively and the electron-impurity scattering leads to an increase in the SDT. This feature is different for high temperatures as shown in Fig. 3(b), where the SDT increases with the increase of the impurity density. The reason is understood as the reduction of the inhomogeneous broadening for high temperature (see more detail in the next section). Therefore, the second effect mentioned above dominants. Consequently, the scattering tends to reduce the dephasing and the dephasing time increases with the concentration of the impurities.

### C. The temperature dependence of the spin dephasing time

Above we discussed the dependence of spin dephasing on initial spin polarization for different temperatures. Now we turn to the temperature dependence of the SDT under different initial spin polarizations. From Fig. 3(a) and (b) in Sec. III(B), one can see that for small polarization, the SDT increases with the temperature. Whereas in high polarized region, the SDT decreases with the temperature. For moderate polarization, the temperature dependence is too complicated to be described by a monotonic function of temperature. For certain condition, the SDT is insensitive with the temperature, e.g. the SDT is almost unchanged with the temperature when the polarization  $P = 75\%$  and  $N_i = 0.1N_e$ .

To see more detail of how the spin dephasing depends on the temperature, we replot the SDT shown in Fig. 3 as a function of the temperature for different impurity levels and different spin polarizations in Fig. 5(a) and (b). It is seen from the figure that, for low polarization, the SDT increases systematically with the temperature for all impurity levels. This property is *opposite* to the results of earlier simplified treatments of the DP effect, where it was predicted that the spin lifetime decreases with the increase of temperature in the 2D system.<sup>41,43</sup> The SDT based on the simplified model is given by<sup>23,41,42</sup>

$$\frac{1}{\tau} = \frac{\int_0^\infty dE_k (f_{k\frac{1}{2}} - f_{k-\frac{1}{2}}) \Gamma(k)}{\int_0^\infty dE_k (f_{k\frac{1}{2}} - f_{k-\frac{1}{2}})}, \quad (10)$$

in which

$$\begin{aligned} \Gamma(k) = 2\tau_1(k) & \left[ (\gamma\langle k_z^2 \rangle)^2 k^2 - \frac{1}{2}\gamma\langle k_z^2 \rangle k^4 \right. \\ & \left. + \frac{1 + \tau_3(k)/\tau_1(k)}{16} \gamma^2 k^6 \right] \end{aligned} \quad (11)$$

and

$$\tau_n^{-1}(k) = \int_0^{2\pi} \sigma(E_k, \theta) [1 - \cos(n\theta)] d\theta. \quad (12)$$

$\sigma(E_k, \theta)$  stands for scattering cross-section. For comparison, we plot the SDT predicated by the earlier model and by our present many-body theory in the inset of Fig. 5(a). From the inset one can see that the SDT predicated by the earlier model is about one order of magnitude larger than the one predicated by our theory. In the mean time, the SDT of the earlier mode drops dramatically with the increase of the temperature. Nevertheless, in our many-body treatment, it rises slightly with the temperature.

The recent experiments show that the SDT in  $n$ -type quantum wells increases slightly with the increase of temperature,<sup>44</sup> or is almost unchanged with the temperature.<sup>45</sup> Moreover, it has been reported very recently that there is a big discrepancy between the earlier simplified treatment of the DP effect and the experiment on the SDT. It is shown that the theoretical SDT is about one order of magnitude larger than the experiment data in  $n$ -type bulk GaAs.<sup>46</sup>

It is seen that our many-body result is better than the earlier simplified treatments both qualitatively and quantitatively. The reason that our model is more precise than the earlier one lies on the fact that the earlier model is based on the single particle picture which does not count for the dephasing due to the inhomogeneous broadening inherited in the DP term, which is the result of many body effect.<sup>21,22,23,24,25</sup> By comparing the theoretical SDT predicated by the two models, we can see that the spin dephasing due to the inhomogeneous broadening is much more important. In the case we calculated, the spin dephasing is dominated by the inhomogeneous broadening. Therefore, it is easy to understand why the earlier simplified treatment of the DP mechanism gives much slower spin dephasing.

The temperature dependence of the SDT can be easily understood when the spin dephasing due to inhomogeneous broadening is taken into account: When the temperature increases, the inhomogeneous broadening is reduced as the electrons are distributed to the wider  $k$ -states. As a result, the number of electron occupation on each  $\mathbf{k}$  state is reduced. It is further noted that this reduction is mild as function of the temperature. Therefore, the temperature dependence is quite mild unless it is within the regime of anomalous peak.

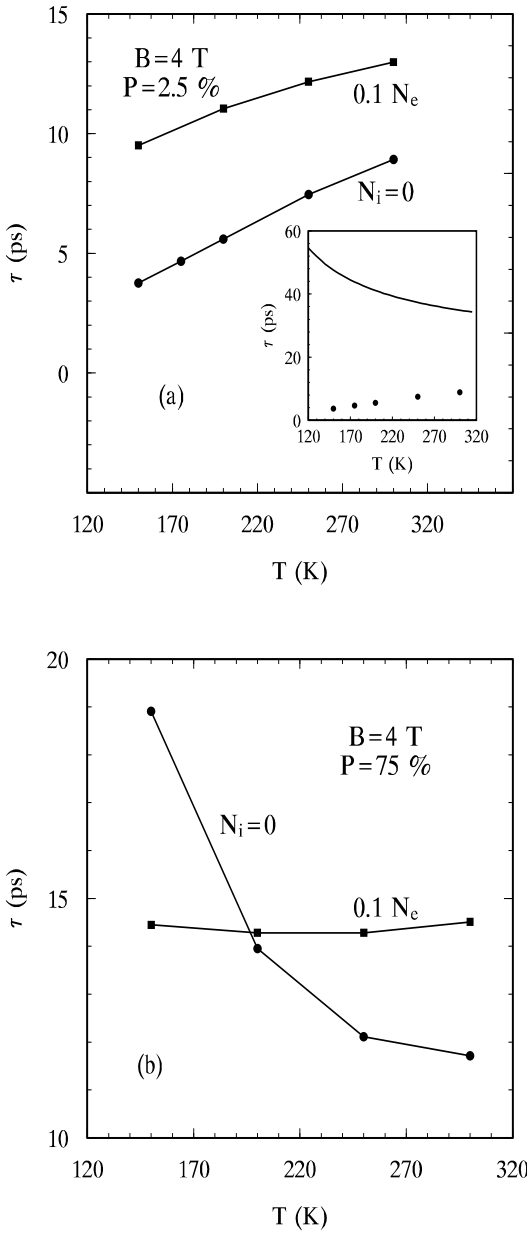


FIG. 5. Spin dephasing time  $\tau$  versus the temperature  $T$  for GaAs QW's with spin polarization  $P = 2.5\%$  (a) and  $P = 75\%$  (b) under two different impurity levels. Circle ( $\bullet$ ):  $N_i = 0$ ; Square ( $\blacksquare$ ):  $N_i = 0.1 N_e$ . The lines are plotted for eye aid. The SDT predicated by the simplified treatment of DP term (solid curve) and our model (circle) for  $N_i = 0$  is plotted in the inset of (a) for comparison.

In the region where HF term is important, in addition to the above mentioned two effects of the temperature acting on the spin dephasing, the temperature dependence of HF term should also be taken into account when we study the temperature dependence of the spin dephasing. Generally, the temperature dependence of SDT due to the combination of these three effects is too complicate to be described by a monotonic function. We replot the

SDT as a function of the temperature in Fig. 5(b), for the special polarization  $P = 75\%$ , which is near the anomalous peak shown in Fig. 3(a). We can see that due to the reduction of the HF term, the resonance is removed and the SDT drops dramatically with the increase of the temperature in the impurities free sample. While for the system with impurity concentration  $N_i = 0.1 N_e$ , the HF term is not as important as in the impurities free sample, and the SDT is insensitive to the temperature.

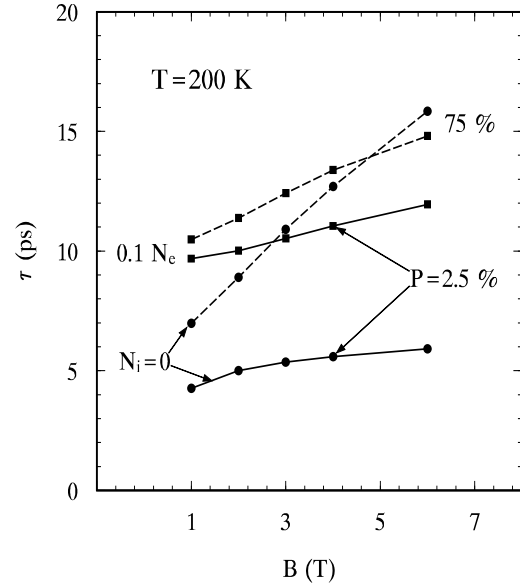


FIG. 6. Spin dephasing time  $\tau$  versus the applied magnetic field for GaAs QW's for different spin polarizations and different impurity levels. Solid curve with circle dots:  $N_i = 0, P = 2.5\%$ ; Solid curve with square dots:  $N_i = 0.1 N_e, P = 2.5\%$ ; Dashed curve with circle dots:  $N_i = 0, P = 75\%$ ; Dashed curve with square dots:  $N_i = 0.1 N_e, P = 75\%$ .

#### D. Magnetic field dependence of the spin dephasing

We now investigate the magnetic field dependence of the spin dephasing. In Fig. 6, we plot the SDT versus the applied magnetic field for different impurity levels and different spin polarizations. It is seen that for all the cases we study, the SDT increases with the magnetic field. This is because in the presence of a magnetic field, the electron spins undergo a Larmor precession around the magnetic field. This precession suppresses the precession about the effective magnetic field  $\mathbf{h}(\mathbf{k})$ .<sup>13,47</sup> Therefor the SDT increases with the magnetic field. It is pointed out that in 3D electron gas, the magnetic field also forces electrons to precess around it. This precession introduces additional symmetry in the momentum space that limits the  $\mathbf{k}$ -space available to the DP effect which is anisotropic in it.<sup>13,21,47</sup> This can further reduce the spin dephasing. However, it is expected that this effect in the 2D case is less effective than the 3D case as in  $z$ -direction the

momentum is quantized and the momentum precession around the magnetic field should be suppressed.

In additional to the above mentioned effect of the magnetic field on spin dephasing, one can further see from Fig. 6, that for large polarization, the magnetic field also enhances the HF term. As we mentioned before, for large polarization, the contribution from the HF term is important. Increase of the HF term serves as additional magnetic field which further suppresses the effect of the DP term  $\mathbf{h}(\mathbf{k})$ , and therefore results in a faster rise in the  $\tau$ - $B$  curve. To reveal more concrete about the combining effect of the magnetic field and the HF term on spin dephasing, we plot the SDT as a function of polarization in Fig. 7. It is shown that the rise in the  $\tau$ - $P$  curve increases with the magnetic field. Moreover, the position of the peak in  $\tau$ - $P$  shifts to a larger polarization. This is understood that, it needs a larger HF term, and hence a larger spin polarization, to achieve the resonance condition when the magnetic field increases. When the magnetic field is raised to 8 T, it is no longer possible to form the resonance for all of the polarization. As a result the SDT increases uniquely with the polarization and there is no peak in the  $\tau$ - $P$  curve.

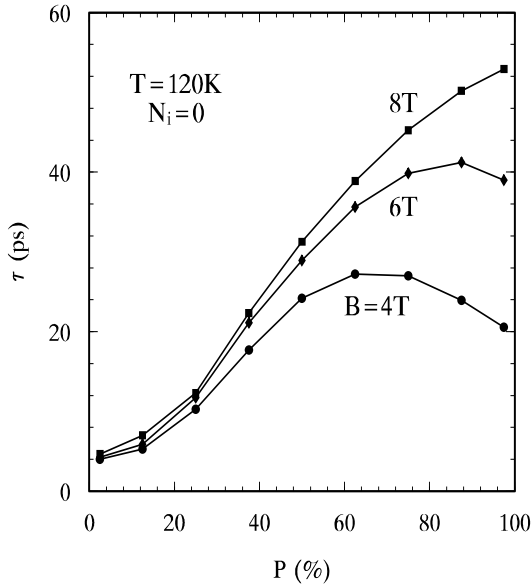


FIG. 7. Spin dephasing time  $\tau$  versus the polarization for GaAs QW's at different magnetic field. Circle (●):  $B=4$  T; Diamond (◆):  $B=6$  T; Square (■):  $B=8$  T. The lines are plotted for the aid of eyes.

#### E. Electron density dependence of spin dephasing

We now investigate the electron density dependence of the spin dephasing. In Fig. 8 we plot the SDT as a function of the electron density for both low and high spin polarization in a GaAs QW. It can be seen from the figure that for low polarization, the SDT decreases with

electron density from 7.8 ps for  $N_e = 1 \times 10^{11} \text{ cm}^{-2}$  to 2 ps for  $N_e = 40 \times 10^{11} \text{ cm}^{-2}$ . This is because with the increase of the electron density, more electrons are distributed at large momentum states and strengthen the DP effect as the DP term increases with the momentum. Whereas for high spin polarization, the SDT first increases from 12.6 ps of  $N_e = 1 \times 10^{11} \text{ cm}^{-2}$  to 14.3 ps of  $N_e = 2 \times 10^{11} \text{ cm}^{-2}$ . However, when the electron density is further raised, the SDT drops again. This is because when the electron density increases, both the HF term and the DP effect increase. When the electron density is increased to a right one, the resonance condition of the HF term and DP effect as well as the magnetic field is achieved. If the electron density is raised too much, the resonance condition is lost and the decrease of SDT due to the enhance of DP effect dominates. Therefore, SDT decreases again with the increase of the electron density.

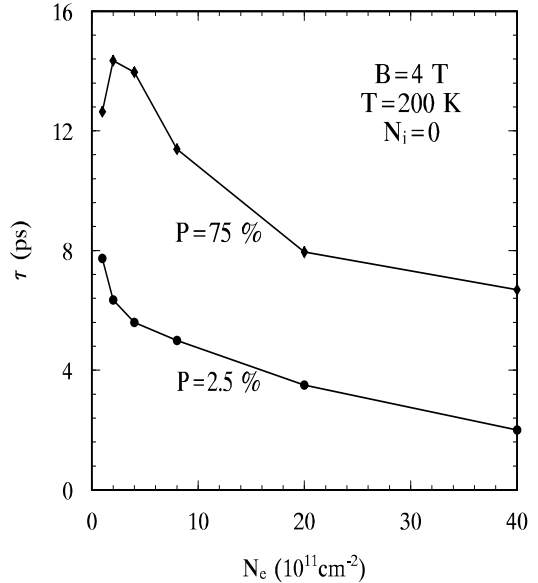


FIG. 8. Spin dephasing time  $\tau$  versus the total electron density  $N_e$  for a GaAs QW with  $T = 200$  K,  $B = 4$  T,  $N_i = 0$  and  $P = 2.5$  % (●) and  $P = 75$  % (◆). The lines are plotted for the aid of eyes.

#### IV. CONCLUSION

In conclusion, we have performed a systematic investigation of the DP effect on the spin dephasing of  $n$ -typed GaAs QW's under moderate magnetic fields in Voigt configuration. Based on the nonequilibrium Green's function theory, we derived a set of kinetic Bloch equations for a two-spin-band model. This model includes the electron-phonon, electron-impurity scattering as well as the electron-electron interaction. By numerically solving the kinetic Bloch equations, we study the time evolution of electron densities in each spin band and the spin coherence – the correlation between spin-up and -down

bands. The spin dephasing time is calculated from the slope of the envelope of the time evolution of the incoherently summed spin coherence. We therefore are able to study in detail how this dephasing time is affected by spin polarization, temperature, impurity level, magnetic field and electron density. Different from the earlier studies on spin dephasing based on the single particle model which only considers the effective SF scattering, our theory also takes account of the contribution of many-body effect on the spin dephasing.<sup>21,22,23,24,25</sup> In fact, for the  $n$ -typed semiconductors and the spin polarization studied in the experiments, this many-body dephasing effect is even more important than the effective spin-flipping scattering as it is one order of magnitude larger than the later. Equally remarkable is that, as we include all the scattering, especially the Coulomb scattering in our many-body theory, now we are able to calculate the spin dephasing with extra large (up to 100 %) initial spin polarization.

It is discovered that the SDT increases with the initial spin polarization. Moreover, for low impurity level and low temperature, there is a giant anomalous resonant peak in the curve of the SDT versus the initial spin polarization. This resonant peak moves to high spin polarization and its magnitude is fast reduced (enhanced) until the whole resonance disappears if one increases the impurity density and/or the temperature (the magnetic field). It is discovered that this anomalous resonance peak originates from the HF contribution of the electron-electron Coulomb interaction. Under the right spin polarization, the contribution of HF term may reach the magnitude comparable to the contribution of the DP term as well as the magnetic field in the coherent part of the Bloch equation and reduces the anisotropy caused by the DP effect—consequently reduces the spin dephasing. As the resonance is the combined effects of the HF term, the DP term and the magnetic field, the magnitude and position of the resonance peak are affected by all the factors that can alert the magnitude of the HF term, such as temperature, impurity scattering, magnetic field as well as the electron density: For a given impurity concentration, when the temperature increases, the HF term reduces. Consequently the  $\tau$ - $P$  curve is smoothed and the peak position is moved to higher spin polarization; For impurities free samples, if the the temperature is raised to 200 K, the HF term is reduced too much to form a resonance and the anomalous peak disappears; The same situation happens when the impurity level increases at a given temperature as the scattering also lowers the HF term. When the impurity level is raised to  $0.1N_e$  there is no resonance in the temperature region we studied; While the increase of the magnetic field enhances the HF term and results in a faster increase of the SDT as well as a higher resonant peak in  $\tau$ - $P$  curve. Moreover, as the magnetic field becomes larger, it needs a larger HF term and hence a larger polarization in order to achieve the resonant condition. Therefore the peak position is also moved to higher polarization.

For low spin polarized regime, the SDT increases when the temperature rises. This is contrary to the result of earlier simplified single-particle calculation where the SDT always decreases with the increase of the temperature. Moreover, the SDT predicted by our many-body calculation is one order of magnitude faster than the earlier result. We show that our results are in agreement with the experiments not only qualitatively but also quantitatively. The physics of this feature is due to the additional many-body spin dephasing channel due to the inhomogeneous broadening provided by the DP term, which by combining with the SC scattering also causes spin dephasing. In the situation we studied, the spin dephasing is dominated by the many-body dephasing effect. With the increase of the temperature, the inhomogeneous broadening reduces and the SDT increases.

The effect of the electron-impurity scattering on the spin dephasing is also studied. We find that for low spin polarized electrons, the SDT decreases as the impurity concentration increases from 0 to  $0.01N_e$  when the temperature is 120 K. If the impurity concentration is further raised to  $0.1N_e$ , the SDT increases again. Whereas when the temperature rises to 200 K the SDT always increases with the impurity concentration. This interesting property is due to the dual roles the scattering plays in the spin dephasing. On the one hand, the scattering enhances spin dephasing as it provides additional spin dephasing channel. On the other hand, it can also redistribute the electrons to an isotropic state which in turn reduces the spin dephasing. In the low temperature regime, the inhomogeneous broadening introduced by the DP term is large and also the isotropic effect caused by the scattering is less effective. Therefore when the impurities are first introduced, the spin dephasing is enhanced by the electron-impurity scattering. When the impurity concentration is further raised to  $0.1N_e$ , the second effect of the scattering dominates and thus reduces the spin dephasing. While in high temperature region, the inhomogeneous broadening reduces. As a result the first effect becomes less important and the SDT increases with the increase of the impurity level.

In high spin polarization region, in additional to the above mentioned dual roles the scattering plays in the spin dephasing, the scattering also affects the HF term. This brings more complication in the study of the spin dephasing. Usually the SDT can not be described a monotonic function of the temperature or the impurity concentration in high polarization region. For a specially polarization  $P = 75\%$ , which is near the resonance peak in low temperature and impurities free samples, the SDT decreases dramatically with the temperature as the resonance is removed when the temperature increases. Whereas when the impurity concentration is  $0.1N_e$ , the SDT is insensitive to the temperature.

As the magnetic field causes the electron spins to precess about it, this precession will suppress the precession about the effective magnetic field  $\mathbf{h}(\mathbf{k})$  originated

from the DP effect. As a result the spin dephasing is reduced. The magnetic field also enhances the HF term, which serves as an additional magnetic field and further suppresses the DP effect. Therefore, the  $\tau$ - $B$  curve gets a faster increase in the high polarization region. Our calculation also shows that when the electron density increases, the SDT decreases. This is because with the increasing of the electron density more electrons are distributed at larger momentum state and consequently the DP term is strengthened.

In summary we have performed a thorough investigation of the spin dephasing in  $n$ -typed GaAs QW's. Many new features which have not been investigated experimentally are predicted in a wide range of parameters.

## ACKNOWLEDGMENTS

MWW is supported by the “100 Person Project” of Chinese Academy of Sciences and Natural Science Foundation of China under Grant No. 10247002. He is also partially supported by Cooperative Excitation Project of ERATO (JST).

\* Author to whom correspondence should be addressed.  
Email: mwwu@ustc.edu.cn.

<sup>1</sup> T. C. Damen, L. Vina, J. E. Cunningham, J. Shah, and L. J. Sham, Phys. Rev. Lett. **67**, 3432 (1991).

<sup>2</sup> J. Wagner, H. Schneider, D. Richards, A. Fischer, and K. Ploog, Phys. Rev. B **47**, 4786 (1993).

<sup>3</sup> J. J. Baumberg, S. A. Crooker, D. D. Awschalom, N. Samarth, H. Luo, and J. K. Furdyna, Phys. Rev. Lett. **72**, 717 (1994); Phys. Rev. B **50**, 7689 (1994).

<sup>4</sup> A. P. Heberle, W. W. Rühle, and K. Ploog, Phys. Rev. Lett. **72**, 3887 (1994).

<sup>5</sup> C. Buss, R. Frey, C. Flytzanis, and J. Cibert, Solid State Commun. **94**, 543 (1995).

<sup>6</sup> S. A. Crooker, J. J. Baumberg, F. Flack, N. Samarth, and D. D. Awschalom, Phys. Rev. Lett. **77**, 2814 (1996); Phys. Rev. B **56**, 7574 (1997).

<sup>7</sup> C. Buss, R. Pankoke, P. Leisching, J. Cibert, R. Frey, and C. Flytzanis, Phys. Rev. Lett. **78**, 4123 (1997).

<sup>8</sup> J. M. Kikkawa, I. P. Smorchkova, N. Samarth, and D. D. Awschalom, Science **277**, 1284 (1997).

<sup>9</sup> J. M. Kikkawa and D. D. Awschalom, Nature **397**, 139 (1998).

<sup>10</sup> J.M. Kikkawa and D.D. Awschalom, Phys. Rev. Lett. **80**, 4313 (1998).

<sup>11</sup> H. Ohno, Science **281**, 951 (1998).

<sup>12</sup> Y. Ohno, R. Terauchi, T. Adachi, F. Matsukura, and H. Ohno, Phys. Rev. Lett. **83**, 4196 (1999).

<sup>13</sup> F. Meier and B. P. Zakharchenya (Eds), *Optical Orientation*, (North-Holland, Amsterdam, 1984).

<sup>14</sup> A. G. Aronov, G. E. Pikus, and A. N. Titkov, Zh. Eksp. Teor. Fiz. **84**, 1170 (1983) [Sov. Phys.-JETP **57**, 680 (1983)].

<sup>15</sup> Y. Yafet, Phys. Rev. **85**, 478 (1952).

<sup>16</sup> R. J. Elliot, Phys. Rev. **96**, 266 (1954).

<sup>17</sup> M. I. D'yakonov and V. I. Perel', Zh. Eksp. Teor. Fiz. **60**, 1954 (1971) [Sov. Phys.-JETP **38**, 1053 (1971)].

<sup>18</sup> G. L. Bir, A. G. Aronov, and G. E. Pikus, Zh. Eksp. Teor. Fiz. **69**, 1382 (1975) [Sov. Phys.-JETP **42**, 705 (1975)].

<sup>19</sup> Haug and A. P. Jauho, *Quantum Kinetics in Transport and Optics of Semiconductors*, (Springer-Verlag, Berlin 1996).

<sup>20</sup> M. W. Wu and H. Metiu, Phys. Rev. B **61**, 2945 (2000).

<sup>21</sup> M. W. Wu and C. Z. Ning, Phys. Status Solidi B **222**, 523 (2000).

<sup>22</sup> M. W. Wu and M. Kuwata-Gonokami, Solid State Commun. **121**, 509 (2002).

<sup>23</sup> M. W. Wu, J. Phys. Soc. Jap. **70**, 2195 (2001).

<sup>24</sup> M. W. Wu and C. Z. Ning, Eur. Phys. J. B **18**, 373 (2000).

<sup>25</sup> M. W. Wu, J. Supercond.: Incorporating Novel Mechanism **14**, 245 (2001); cond-mat/0109258.

<sup>26</sup> G. Dresselhaus, Phys. Rev. **100**, 580 (1955).

<sup>27</sup> Yu. A. Bychkov and E.I. Rashba, J. Phys. C **17**, 6039 (1984).

<sup>28</sup> Yu A. Bychkov and E.I. Rashba, Sov. Phys. JETP Lett. **39**, 78 (1984).

<sup>29</sup> R. Eppenga and M. F. H. Schuurmans, Phys. Rev. B **37**, 10923 (1988).

<sup>30</sup> E. L. Ivchenko and G. E. Pikus, *Superlattices and Other Heterostructures*, (Springer, Berlin, 1995).

<sup>31</sup> G. D. Mahan, *Many-particle Physics*, (Plenum, New York 1981).

<sup>32</sup> T. Kuhn and F. Rossi, Phys. Rev. Lett. **69**, 977 (1992).

<sup>33</sup> O. Madelung, M. Schultz, and H. Weiss (eds.), *Numerical Data and Functional Relationships in Science and Technology*, Landolt-Börnstein, New Series, Vol. 17, (Springer-Verlag, Berlin 1982).

<sup>34</sup> C. T. Liang, C. G. Smith, M. Y. Simmons, and D. A. Ritchie, Phys. Rev. B **64**, 233319 (2001).

<sup>35</sup> I. L. Drichko, A. M. Diakonov, V. V. Preobrazenskii, I. Yu. Smirnov, and A. I. Toropov, Physica B **284**, 1732 (2000).

<sup>36</sup> A. Usher, R. J. Nicholas, J. J. Harris, and C. T. Foxon, Phys. Rev. B **41**, 1129 (1990).

<sup>37</sup> R. J. Nicholas, R. J. Haug, K. V. Klitzing, and W. Weimann, Phys. Rev. B **37**, 1294 (1988).

<sup>38</sup> F. F. Fang and P. J. Sitles, Phys. Rev. **174**, 823 (1968).

<sup>39</sup> It is noted that the experimental results of the  $g$ -factor in the direction perpendicular to the QW growth axis used in the present computation are measured in the low temperature regime. There is no experimental result of the high temperature case. However, if the  $g$ -factor for the high temperature regime turns out to be close to the bulk value, *ie.*, 0.44, then the conclusion of the present computation should be reinterpreted to be the result in the high magnetic field regime, which means, *eg.*  $B = 4$  T in the present case then corresponds to the high field of 59 T. This high field can be achieved experimentally by the pulsed magnetic field with the stable duration of the field pulse being orders of magnitude longer than the SDT [ M. Respaud, A. Llobet, C. Frontera, C. Ritter, J. M. Broto, H. Rakoto, M. Goiran, and J. L. Garcia-Munoz, Phys. Rev. B **61**, 9014 (2000); V.

A. Kulbachinskii, N. Miura, H. Nakagawa, H. Arimoto, T. Ikaida, P. Lostak, and C. Drasar, Phys. Rev. B **59**, 15733 (1999)]. Experiments are needed to determine the real  $g$ -factor for the high temperature regime.

<sup>40</sup> M. M. Glazov and E. L. Ivchenko, Pis'ma Zh. Eksp. Teor. Fiz. **75**, 476 (2002) [JETP Lett. **75**, 403 (2002)].

<sup>41</sup> N. S. Averkiev, L. E. Golub, and M. Willander, J. Phys.: Cond. Mat. **14**, R271 (2002); Semiconductors **36**, 91 (2002).

<sup>42</sup> W. H. Lau, J. T. Oleberg, and M. E. Flatté: Phys. Rev. B **64**, 161301 (2001).

<sup>43</sup> M. I. Dyakonov and V. Yu. Kachorovskii, Fiz. Tekh. Poluprovodn. **20**, 178 (1986) [Soviet Phys. - Semicond. **20**, 110 (1986)].

<sup>44</sup> D. Hägele, M. Oestreich, W.W. Rühle, J. Hoffmann, S. Wachter, H. Kalt, K. Ohkawa, D. Hommel, Physica B **272**, 338 (1999).

<sup>45</sup> A. Malinowski, R. S. Britton, T. Grevatt, R. T. Harley, D. A. Ritchie, and M. Y. Simmons, Phys. Rev. B **62**, 13034 (2000).

<sup>46</sup> P. H. Song and K. W. Kim, Phys. Rev. B **66**, 035207 (2002).

<sup>47</sup> F. X. Bronold, I. Martin, A. Saxena, and D. L. Smith, cond-mat/0208139.

$\kappa_\infty$	10.8	$\kappa_0$	12.9
$\omega_0$	35.4 meV	$m^*$	0.067 $m_0$
$\Delta$	0.341 eV	$E_g$	1.55 eV

TABLE I. Parameters used in the numerical calculations